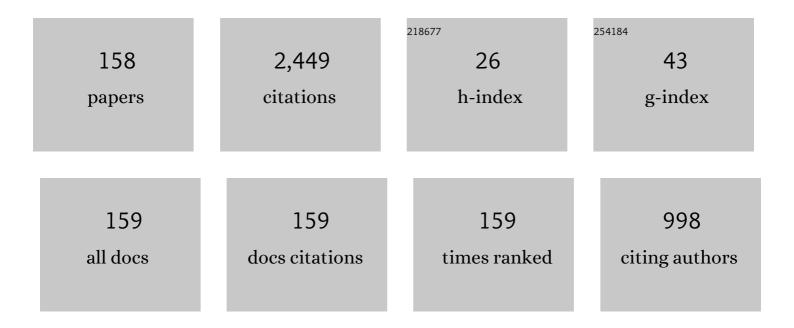
Jixiong Pu

List of Publications by Year in descending order

Source: https://exaly.com/author-pdf/1811976/publications.pdf Version: 2024-02-01



#	Article	IF	CITATIONS
1	Increasing field of view and signal to noise ratio in the quantitative phase imaging with phase shifting holography based on the Hanbury Brown-Twiss approach. Optics and Lasers in Engineering, 2022, 148, 106771.	3.8	20
2	Generation of controllable spectrum in multiple positions from speckle patterns. Optics and Laser Technology, 2022, 149, 107820.	4.6	7
3	Enhancing circularly polarized XUV vortices from bicircular Laguerre-Gaussian fields. Optics Express, 2022, 30, 2636.	3.4	1
4	Influence of slow light effect on trapping force in optical tweezers. Optics Letters, 2022, 47, 710.	3.3	1
5	Broadband High-Efficiency Ultrathin Metasurfaces With Simultaneous Independent Control of Transmission and Reflection Amplitudes and Phases. IEEE Transactions on Microwave Theory and Techniques, 2022, 70, 254-263.	4.6	38
6	High-Q-factor phase-shifted helical fiber Bragg grating by one-step femtosecond laser inscription for high-temperature sensing. Optics Letters, 2022, 47, 1407.	3.3	4
7	Energy Attenuation Prediction of Dye-Doped PMMA Microfibers by Backpropagation Neural Network. IEEE Photonics Journal, 2022, 14, 1-8.	2.0	0
8	Single-Shot On-Axis Fizeau Polarization Phase-Shifting Digital Holography for Complex-Valued Dynamic Object Imaging. Photonics, 2022, 9, 126.	2.0	8
9	Labelâ€free singleâ€shot imaging with onâ€axis phaseâ€shifting holographic reflectance quantitative phase microscopy. Journal of Biophotonics, 2022, 15, e202100400.	2.3	4
10	Recognizing the orbital angular momentum (OAM) of vortex beams from speckle patterns. Science China: Physics, Mechanics and Astronomy, 2022, 65, .	5.1	15
11	Experimental study on frequency doubling of Q-switched partially coherent laser. Optical Review, 2022, 29, 172-177.	2.0	2
12	Efficient Enhancement of Second Harmonic Generation via Noninvasive Modulation. Applied Sciences (Switzerland), 2022, 12, 3962.	2.5	0
13	Upconversion imaging through multimode fibers based on deep learning. Optik, 2022, 264, 169444.	2.9	2
14	Shape measurement of a thin glass plate through analyzing dispersion effects in a white-light scanning interferometer. Optics and Lasers in Engineering, 2021, 139, 106505.	3.8	1
15	Mutual Transfer Learning of Reconstructing Images Through a Multimode Fiber or a Scattering Medium. IEEE Access, 2021, 9, 68387-68395.	4.2	5
16	High-fidelity imaging through multimode fibers via deep learning. JPhys Photonics, 2021, 3, 015003.	4.6	15
17	Highâ€Fidelity Image Reconstruction through Multimode Fiber via Polarizationâ€Enhanced Parametric Speckle Imaging. Laser and Photonics Reviews, 2021, 15, 2000376.	8.7	24
18	Large thickness measurement of glass plates with a spectrally resolved interferometer using variable signal positions. OSA Continuum, 2021, 4, 1792.	1.8	2

#	Article	IF	CITATIONS
19	Near-infrared long-range surface plasmon resonance in a D-shaped honeycomb microstructured optical fiber coated with Au film. Optics Express, 2021, 29, 16455.	3.4	11
20	Image reconstruction through a hollow core fiber via deep learning. Optics Communications, 2021, 488, 126840.	2.1	1
21	Generation of Focal Patterns With Uniform Intensity Distribution From Speckle by Hadamard-Genetic Algorithm. IEEE Photonics Journal, 2021, 13, 1-8.	2.0	3
22	Shape measurement of large thickness glass plates with a white-light scanning interferometer using a compensation glass and a fixed reference surface. Engineering Research Express, 2021, 3, 025044.	1.6	0
23	What are the traveling waves composing the Hermite-Gauss beams that make them structured wavefields?. Optics Express, 2021, 29, 29068.	3.4	12
24	Non-invasive imaging through dynamic scattering layers via speckle correlations. Optical Review, 2021, 28, 557-563.	2.0	8
25	Sensitivity Enhanced Refractive Index Fiber Sensor Based on Long-Range Surface Plasmon Resonance in SiO2-Au-TiO2 Heterostructure. Photonics, 2021, 8, 379.	2.0	8
26	Measurement of phase refractive index directly from phase distributions detected with a spectrally resolved interferometer. Applied Optics, 2021, 60, 10009.	1.8	2
27	A wavefront division multiplexing holographic scheme and its application in looking through diffuser. New Journal of Physics, 2021, 23, 113034.	2.9	13
28	Quantitative phase recovery in ghost imaging. , 2021, , .		3
29	Reconstructing images of two adjacent objects passing through scattering medium via deep learning. Optics Express, 2021, 29, 43280.	3.4	19
30	Quantitative Analysis of Structural Parameters Importance of Helical Temperature Microfiber Sensor by Artificial Neural Network. IEEE Access, 2021, 9, 148156-148163.	4.2	6
31	Recovery and Characterization of Orbital Angular Momentum Modes with Ghost Diffraction Holography. Applied Sciences (Switzerland), 2021, 11, 12167.	2.5	4
32	Investigation on Intracavity SHG With Controllable Coherence in a Degenerate Laser. IEEE Journal of Quantum Electronics, 2020, 56, 1-6.	1.9	3
33	A dual-scanning white-light interferometer for exact thickness measurement of a large-thickness glass plate. Measurement Science and Technology, 2020, 31, 045009.	2.6	2
34	Intracavity generated visible self-reconstructing Bessel-like laser beams by thermal effect. Optics Communications, 2020, 458, 124823.	2.1	1
35	Imaging reconstruction through strongly scattering media by using convolutional neural networks. Optics Communications, 2020, 477, 126341.	2.1	17
36	Bragg Grating Assisted Sagnac Interferometer in SiO2-Al2O3-La2O3 Polarization-Maintaining Fiber for Strain–Temperature Discrimination. Sensors, 2020, 20, 4772.	3.8	5

#	Article	IF	CITATIONS
37	Complex field measurement in a single pixel hybrid correlation holography. Journal of Physics Communications, 2020, 4, 045009.	1.2	3
38	A metasurfaceâ€enabled wideband highâ€gain dualâ€circularlyâ€polarized Fabryâ€Perot resonator antenna. Microwave and Optical Technology Letters, 2020, 62, 3195-3202.	1.4	6
39	Direct generation of visible vortex Hermite-Gaussian modes in a diode-pumped Pr:YLF laser. Optics and Laser Technology, 2020, 131, 106389.	4.6	6
40	1 Bit Electronically Reconfigurable Folded Reflectarray Antenna Based on p-i-n Diodes for Wide-Angle Beam-Scanning Applications. IEEE Transactions on Antennas and Propagation, 2020, 68, 6806-6810.	5.1	74
41	Polarization Transmission Matrix for Completely Polarization Control of Focal Spots in Speckle Field of Multimode Fiber. IEEE Journal of Selected Topics in Quantum Electronics, 2020, 26, 1-5.	2.9	10
42	Impact of Nonlinear Kerr Effect on the Focusing Performance of Optical Lens with High-Intensity Laser Incidence. Applied Sciences (Switzerland), 2020, 10, 1945.	2.5	1
43	Imaging of polarimetric-phase object through scattering medium by phase shifting. Optics Express, 2020, 28, 8145.	3.4	16
44	Kepler's law for optical beams. Optics Express, 2020, 28, 31979.	3.4	5
45	Phase shifting digital holography with the Hanbury Brown–Twiss approach. Optics Letters, 2020, 45, 212.	3.3	29
46	Energy losses and fluorescent efficiency of RhB-doped polymer microfibers via optical waveguiding excitation. Applied Optics, 2020, 59, 4542.	1.8	1
47	Backpropagation neural network assisted concentration prediction of biconical microfiber sensors. Optics Express, 2020, 28, 37566.	3.4	6
48	Ghost diffraction holographic microscopy. Optica, 2020, 7, 1697.	9.3	35
49	Focusing and polarized modulation of a laser passing through a multi-core fiber. Optical Review, 2019, 26, 531-536.	2.0	1
50	Detecting the Extremely Small Angle of an Axicon by Phase-Shifting Digital Holography. Applied Sciences (Switzerland), 2019, 9, 3959.	2.5	1
51	Visually Adjusting Coupling Conditions in Light-Emitting Micro-Components. IEEE Photonics Technology Letters, 2019, 31, 1425-1428.	2.5	5
52	Use of Scattering Layer as a Programmable Spectrum Filter. IEEE Journal of Quantum Electronics, 2019, 55, 1-6.	1.9	5
53	Scintillation index of double vortex beams in turbulent atmosphere. Optik, 2019, 181, 571-574.	2.9	14
54	Control the normalized polarization ratio of a focal spot in speckle field formed by non-polarization-maintaining multimode fiber. Journal of Optics (United Kingdom), 2019, 21, 045704.	2.2	1

#	Article	IF	CITATIONS
55	A 1-Bit Electronically Reconfigurable Reflectarray Antenna in X Band. IEEE Access, 2019, 7, 66567-66575.	4.2	52
56	Highâ€efficiency cross and linearâ€ŧo•ircular polarization converters based on novel frequency selective surfaces. Microwave and Optical Technology Letters, 2019, 61, 2410-2419.	1.4	16
57	Highly accurate field-magnitude extraction of monochromatic light waves under FDTD simulations. Optik, 2019, 179, 848-853.	2.9	3
58	Signal correction by detection of scanning position in a white-light interferometer for exact surface profile measurement. Applied Optics, 2019, 58, 3548.	1.8	20
59	Determining topological charge based on an improved Fizeau interferometer. Optics Express, 2019, 27, 12774.	3.4	41
60	Speckle-field digital polarization holographic microscopy. Optics Letters, 2019, 44, 5711.	3.3	14
61	Ni 3 Se 2 electrodes for high performance lithium-ion and sodium-ion batteries. Materials Letters, 2018, 220, 86-89.	2.6	18
62	Accuracy and von Neumann stability of several highly accurate FDTD approaches for modelling Debyeâ€ŧype dielectric dispersion. IET Microwaves, Antennas and Propagation, 2018, 12, 211-216.	1.4	2
63	On the Optimal Switch Functions for Fast FDTD Monochromatic Lightwave Generation. IEEE Photonics Technology Letters, 2018, 30, 115-118.	2.5	0
64	Tailoring and analysis of vectorial coherence. Journal of Optics (United Kingdom), 2018, 20, 125605.	2.2	4
65	Needle Beam Generated by a Laser Beam Passing Through a Scattering Medium. IEEE Photonics Journal, 2018, 10, 1-8.	2.0	5
66	Experimental investigation on a nonuniformly correlated partially coherent laser. Applied Optics, 2018, 57, 4381.	1.8	3
67	Generation of focal pattern with controllable polarization and intensity for laser beam passing through a multi-mode fiber. Optics Express, 2018, 26, 7693.	3.4	14
68	Dual-cavity digital laser for intra-cavity mode shaping and polarization control. Optics Express, 2018, 26, 18182.	3.4	13
69	Experimental investigation on optical vortex tweezers for microbubble trapping. Open Physics, 2018, 16, 383-386.	1.7	8
70	Exact surface profile measurement without subtracting dispersion phase through Fourier transform in a white-light scanning interferometer. Applied Optics, 2018, 57, 894.	1.8	7
71	Propagation Characteristics of High-Power Vortex Laguerre-Gaussian Laser Beams in Plasma. Applied Sciences (Switzerland), 2018, 8, 665.	2.5	6
72	Effects of beam coherence on the focusing of laser beam through scattering media. Applied Physics B: Lasers and Optics, 2018, 124, 1.	2.2	1

#	Article	IF	CITATIONS
73	High-energy nanosecond radially polarized beam output from Nd:YAG amplifiers. Optical Review, 2017, 24, 188-192.	2.0	6
74	Modeling the ponderomotive interaction of high-power laser beams with collisional plasma: the FDTD-based approach. Optics Express, 2017, 25, 8440.	3.4	7
75	Generation of partially coherent beams with controllable time-dependent coherence. Optical Engineering, 2017, 56, 1.	1.0	0
76	Generation of stochastic electromagnetic beams with complete controllable coherence. Optics Express, 2016, 24, 21587.	3.4	18
77	Amplification of vortex beam in Nd:YAG power amplifiers. , 2016, , .		0
78	Second harmonic generation of off axial vortex beam in the case of walk-off effect. Optics Communications, 2016, 370, 267-275.	2.1	1
79	Focusing light into desired patterns through turbid media by feedback-based wavefront shaping. Applied Physics B: Lasers and Optics, 2016, 122, 1.	2.2	30
80	Generation of stochastic electromagnetic beams with controllable coherence. , 2016, , .		0
81	A coordinate transformation method for calculating the 3D light intensity distribution in ICF hohlraum. Optics Communications, 2016, 368, 123-128.	2.1	0
82	High-Energy Nanosecond Optical Vortex Output From Nd:YAG Amplifiers. IEEE Photonics Technology Letters, 2016, 28, 1271-1274.	2.5	10
83	Tight focusing induces pulse delay and pulse compression of double-ring-shaped radially polarized ultrashort light pulses. Journal of Modern Optics, 2016, 63, 697-703.	1.3	0
84	Elegant Cartesian Laguerre–Hermite–Gaussian laser cavity modes. Optics Letters, 2015, 40, 1105.	3.3	8
85	Devil's lens optical tweezers. Optics Express, 2015, 23, 8190.	3.4	26
86	Propagation properties of off axial partially coherent vortex beam. Optics Communications, 2015, 357, 172-176.	2.1	2
87	Measuring the intensity fluctuation of partially coherent radially polarized beams in atmospheric turbulence. Optics Express, 2014, 22, 18278.	3.4	21
88	Spectral anomalies by superposition of polychromatic Gaussian beam and Gaussian vortex beam. Optics Express, 2014, 22, 20193.	3.4	6
89	The cross correlation function of partially coherent vortex beam. Optics Express, 2014, 22, 1350.	3.4	17
90	Pulse delay and pulse compression of ultrashort light pulses in tight focusing. Optics Communications, 2014, 332, 164-168.	2.1	7

#	Article	IF	CITATIONS
91	Theoretical modeling on resonating the second harmonic for ultraviolet laser generation. Journal of Modern Optics, 2014, 61, 1152-1157.	1.3	0
92	Radiation forces on a Rayleigh particle by a highly focused elliptically polarized beam. Journal of Modern Optics, 2014, 61, 954-960.	1.3	2
93	The effect on on-axis degree of polarization of stochastic vortex light beams by degree of coherence. Optics Communications, 2014, 324, 63-68.	2.1	0
94	Propagation properties and self-reconstruction of azimuthally polarized non-diffracting beams. Optics Communications, 2013, 294, 36-42.	2.1	9
95	Tight focusing of partially coherent and radiallly polarized vortex beams. Optics Communications, 2013, 295, 5-10.	2.1	14
96	Generating and shifting a spherical focal spot in a 4Pi focusing system illuminated by azimuthally polarized beams. Physics Letters, Section A: General, Atomic and Solid State Physics, 2013, 377, 2231-2234.	2.1	19
97	Propagation of an optical vortex beam through a diamond-shaped aperture. Optics and Laser Technology, 2013, 45, 473-479.	4.6	21
98	Propagation characteristics of a high-power broadband laser beam passing through a nonlinear optical medium with defects. High Power Laser Science and Engineering, 2013, 1, 132-137.	4.6	3
99	Experimental generation of nonuniformly correlated partially coherent light beams. Optics Letters, 2013, 38, 4821.	3.3	42
100	Generation of super-length optical needle by focusing hybridly polarized vector beams through a dielectric interface. Optics Letters, 2012, 37, 3303.	3.3	51
101	Tight Focusing of Light Beams: Effect of Polarization, Phase, and Coherence. Progress in Optics, 2012, 57, 219-260.	0.6	30
102	Radiation forces of a dielectric medium plate induced by a Gaussian beam. Optics Communications, 2012, 285, 1680-1683.	2.1	7
103	Focusing properties of the double-vortex beams through a high numerical-aperture objective. Optics and Laser Technology, 2012, 44, 441-445.	4.6	12
104	Propagation of partially coherent double-vortex beams in turbulent atmosphere. Optics and Laser Technology, 2012, 44, 1780-1785.	4.6	14
105	Polarisation singularities of non-paraxial Gaussian vortex beams diffracted by an annular aperture. Journal of Modern Optics, 2011, 58, 657-664.	1.3	3
106	Investigation on the scintillation reduction of elliptical vortex beams propagating in atmospheric turbulence. Optics Express, 2011, 19, 26444.	3.4	87
107	Tight focusing of a double-ring-shaped, azimuthally polarized beam. Optics Letters, 2011, 36, 2014.	3.3	96
108	Measuring the orbital angular momentum of elliptical vortex beams by using a slit hexagon aperture. Optics Communications, 2011, 284, 2424-2429.	2.1	29

#	Article	IF	CITATIONS
109	Tight focusing properties of linearly polarized Gaussian beam with a pair of vortices. Physics Letters, Section A: General, Atomic and Solid State Physics, 2011, 375, 2958-2963.	2.1	40
110	Tight focusing of spirally polarized vortex beams. Optics and Laser Technology, 2010, 42, 186-191.	4.6	38
111	Spectral and polarization properties of stochastic electromagnetic beams propagating in gain or absorbing media. Optics Communications, 2010, 283, 1693-1706.	2.1	5
112	Nanosecond zero-order pulsed Bessel beam generated from unstable resonator based on an axicon. Optics and Laser Technology, 2010, 42, 941-944.	4.6	4
113	Focusing of a femtosecond vortex light pulse through a high numerical aperture objective. Optics Express, 2010, 18, 10822.	3.4	23
114	Propagation properties of partially coherent radially polarized beam in a turbulent atmosphere. Journal of Modern Optics, 2009, 56, 1296-1303.	1.3	33
115	Beam-spreading and topological charge of vortex beams propagating in a turbulent atmosphere. Optics Communications, 2009, 282, 1255-1259.	2.1	52
116	Focus shaping of cylindrically polarized vortex beams by a high numerical-aperture lens. Optics and Laser Technology, 2009, 41, 241-246.	4.6	73
117	Lens axicon illuminated by polychromatic Gaussian beams for generating uniform focal segments. Optik, 2009, 120, 56-61.	2.9	1
118	Focal shift of the partially coherent vortex beams focused by an aperture lens. Optik, 2009, 120, 574-578.	2.9	2
119	Partially coherent aberrated beam propagating in a turbulent atmosphere. Optik, 2009, 120, 829-834.	2.9	4
120	Propagation of the degree of cross-polarization of a stochastic electromagnetic beam through the turbulent atmosphere. Optics Communications, 2009, 282, 1691-1698.	2.1	40
121	Influence of the comatic aberration of an apertured lens on the focused polychromatic Gaussian beams. Optics and Lasers in Engineering, 2008, 46, 679-686.	3.8	0
122	Effective Fresnel number and focal shifts for focused cylindrical spherical aberrated beams. Optics and Laser Technology, 2008, 40, 742-747.	4.6	0
123	Band gap structure of disordered chiral photonic crystals. Optical and Quantum Electronics, 2008, 40, 757-765.	3.3	1
124	Partially coherent vortex beams focused by an aperture lens with coma. Optical Review, 2008, 15, 259-264.	2.0	0
125	Stochastic electromagnetic vortex beam and its propagation. Physics Letters, Section A: General, Atomic and Solid State Physics, 2008, 372, 2734-2740.	2.1	20
126	Propagation of non-uniformly polarized beams in a turbulent atmosphere. Optics Communications, 2008, 281, 3617-3622.	2.1	17

#	Article	IF	CITATIONS
127	Investigation on z-scan experiment by use of partially coherent beams. Optics Communications, 2008, 281, 326-330.	2.1	4
128	Tightly focusing of linearly polarized vortex beams through a dielectric interface. Optics Communications, 2008, 281, 3421-3426.	2.1	12
129	Propagation of partially coherent Bessel-Gaussian beams in turbulent atmosphere. Optics and Laser Technology, 2008, 40, 820-827.	4.6	74
130	Singularities and spectral changes of Gaussian beams focused by a lens with spherical aberration. Optics and Laser Technology, 2008, 40, 881-889.	4.6	3
131	Focusing of partially coherent Bessel-Gaussian beams through a high-numerical-aperture objective. Optics Letters, 2008, 33, 49.	3.3	89
132	Spectral changes of polychromatic stochastic electromagnetic vortex beams propagating through turbulent atmosphere. Journal of Modern Optics, 2008, 55, 2831-2842.	1.3	5
133	Spectral changes in electromagnetic stochastic beams propagating through turbulent atmosphere. Journal of Modern Optics, 2008, 55, 1199-1208.	1.3	25
134	Effective Fresnel number of diffracting screen illuminated by focused partially coherent beams. Journal of Modern Optics, 2007, 54, 1837-1844.	1.3	0
135	On-axis irradiance distribution of axicons illuminated by spherical wave. Optics and Laser Technology, 2007, 39, 1258-1261.	4.6	6
136	Experimental observation of spectral switch of partially coherent light focused by a lens with chromatic aberration. Optics and Laser Technology, 2007, 39, 1226-1230.	4.6	14
137	Invariance and noninvariance of the spectra of stochastic electromagnetic beams on propogation. Optics Letters, 2006, 31, 2097.	3.3	58
138	Experimental observations of the spectrum of light diffracted at a slit as a secondary source. Optics Communications, 2006, 265, 394-398.	2.1	1
139	Spectral anomalies of focused high order Bessel beams in the neighborhood of focus. Optics Communications, 2006, 266, 413-418.	2.1	6
140	The effect of spherical aberration on singularities and spectral changes of focused beams. New Journal of Physics, 2006, 8, 93-93.	2.9	6
141	Focal shift and focal switch of partially coherent light in dual-focus systems. Optics Communications, 2005, 252, 262-267.	2.1	20
142	Partially coherent bottle beams. Optics Communications, 2005, 252, 7-11.	2.1	33
143	Spectral anomalies in Young's double-slit interference experiment. Optics Express, 2004, 12, 5131.	3.4	81
144	Anomalous behaviors of the Fraunhofer diffraction patterns for a class of partially coherent light. Optics Express, 2003, 11, 339.	3.4	6

#	Article	IF	CITATIONS
145	Three-dimensional intensity distribution of focused annular non-uniformly polarized beams. Journal of Modern Optics, 2002, 49, 1501-1513.	1.3	4
146	Spectral changes and 1 × N spectral switches in the diffraction of partially coherent light by an aperture. Journal of the Optical Society of America A: Optics and Image Science, and Vision, 2002, 19, 339.	1.5	40
147	Spectral shifts of partially coherent beams focused by a lens with chromatic aberration. Optics Communications, 2002, 207, 1-5.	2.1	11
148	Uniform-intensity axicon: A lens coded with a symmetrically cubic phase plate. Optical and Quantum Electronics, 2001, 33, 653-660.	3.3	2
149	Spectral shifts and spectral switches in diffraction of partially coherent light by a circular aperture. IEEE Journal of Quantum Electronics, 2000, 36, 1407-1411.	1.9	55
150	Axial intensity distribution of partially coherent light focused by a lens with spherical aberration. Journal of Modern Optics, 2000, 47, 605-612.	1.3	8
151	Axial intensity distribution of partially coherent light focused by a lens with spherical aberration. Journal of Modern Optics, 2000, 47, 605-612.	1.3	4
152	Spectral shifts and spectral switches of partially coherent light passing through an aperture. Optics Communications, 1999, 162, 57-63.	2.1	172
153	Reshaping gaussian Schell-model beams to uniform profiles by lenses with spherical aberration. Journal of Modern Optics, 1999, 46, 1611-1620.	1.3	8
154	Reshaping Gaussian Schell-model beams to uniform profiles by lenses with spherical aberration. Journal of Modern Optics, 1999, 46, 1611-1620.	1.3	1
155	Beam quality changes of Gaussian Schell-model beams propagating through axicons. Optical and Quantum Electronics, 1998, 30, 265-270.	3.3	2
156	Intensity distribution of Gaussian beams focused by a lens with spherical aberration. Optics Communications, 1998, 151, 331-338.	2.1	22
157	Focusing Gaussian beams by an annular lens with spherical aberration. Journal of Modern Optics, 1998, 45, 239-247.	1.3	13
158	Beam shaping of high-power laser beams by aberrated lenses: numerical simulation. , 0, , .		0